Hysteresis Inhibition for Performance Improvement via Halide Engineering in Perovskite Solar Cells

Victor Ming Rui Xu

Crescent School, North York, Canada
Email: xuvictor12@gmail.com
Manuscript received September 5, 2024; revised September 23, 2024; accepted November 16, 2024; published March 27, 2025

***Abstract*—The ongoing climate and energy crisis have become more prevalent than ever. Photovoltaic (PV) technologies directly convert incident solar radiation into electricity, offering a highly efficient and promising method for harnessing solar energy. Recently, a novel semiconductor known as organic-inorganic hybrid Perovskite Solar Cells (PSCs) has emerged as the most promising candidate for the next generation of PV devices due to their cost-effectiveness, simple fabrication process, and impressive Power Conversion Efficiency (PCE). However, several critical issues still remain, among which, the hysteresis effect is a phenomenon unique to PSCs. It results in unstable power output, misleading PCE, and rapid degradation of the solar device, making it a major challenge hindering the global commercialization of PSCs. Ion migration has been identified as the primary cause of the hysteresis effect in PSCs. As a result, the proposed solution involves the use of halide engineering to perform interfacial modification of the Electron Transport Layer (ETL). The findings revealed a consistent reduction in the hysteresis effect across all modifications, with InF3 emerging as the most effective among the various chemical additives employed in the ETL.**

***Keywords*—climate change, solar energy, solar cell, photovoltaics, perovskite, hysteresis, ion migration, interfacial engineering, halide engineering**

I. Introduction

Our world faces an ongoing climate and energy crisis, driven primarily by rapid population growth and technological development in recent years. These two crises have escalated the greenhouse effect and our energy demands to unprecedented levels. This calls for renewable energy sources to replace conventional fossil fuels, addressing the long-term issues associated with these global crises.

Photovoltaic (PV) technologies directly convert incident solar radiation into electricity, offering a highly efficient and promising method for harnessing solar energy with minimal noise, pollution, moving parts, and intermediate steps. They typically exhibit life-cycle emissions approximately 12 times lower than natural gas and 20 times lower than coal, significantly reducing global greenhouse gas emissions [1].

Recently, a novel semiconductor known as organic-inorganic hybrid Perovskite Solar Cells (PSCs) has emerged as the most promising candidate for the next generation of PV devices [2], being cost-effective, and simple to fabricate devices with impressive Power Conversion Efficiency (PCE). Since their introduction in 2009, they have improved remarkably from a PCE of just 3.8% to 26.1% in 2023, just over a decade later. PSCs now rival the PCE of conventional silicon solar cells, which were introduced in the early 1950s and took over 7 decades to reach a comparable PCE.

In general, PSCs have a chemical formula of ABX_3, where A is typically a monovalent cation such as MA^+, FA^+, or Cs^+, B is typically a divalent metal ion such as Pb^{2+}, Sn^{2+}, and the X anion is typically a halogen ion such as Cl^-, Br^-, I^- or F^- [3]. For instance, the most famous active light-harvesting material is methylammonium lead trihalide ($MAPbX_3$). The device architecture usually consists of five different functional layers, as illustrated in Fig. 1. A Transparent Conductive Oxide (TCO) is applied onto a glass substrate and adopted as the front electrode. The Electron Transport Layer (ETL) and Hole Transport Layer (HTL) are responsible for the extraction, collection, and transportation of electrons and holes, respectively. The perovskite active layer is responsible for light absorption and the initial photoinduced charge separation, after which the generated free charge carriers are then transferred to their corresponding transport layer. Finally, they are collected by the metal back electrode, which is often made of gold.

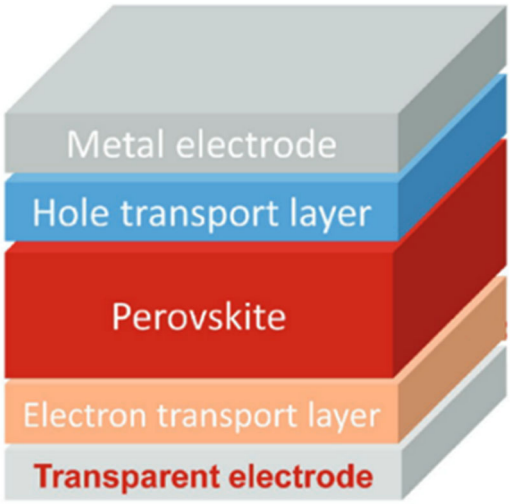

Fig. 1. Schematic graph showing the device architecture of PSCs [4].

Although PSCs have already exceeded the theorized lower PCE limit (10%) for commercialization applications [5], several critical issues still need to be addressed. Among these, the hysteresis effect is perhaps the most important problem regarding PSCs, as it is a phenomenon with minimal prior research and attention.

Researchers utilize the photocurrent density-voltage (*J-V*) measurement to evaluate the power output of a photovoltaic device. It is carried out by recording the current intensity compared to various applied voltages and can be achieved with both voltage scanning directions. However, in a perovskite device, there exists a mismatch of the current density curve when recorded in opposite voltage scanning directions, which is defined as the hysteresis effect, as shown in Fig. 2(b). This discrepancy results in unstable power output and diffi-

doi: 10.18178/ijcea.2025.16.1.834

culty in precisely determining the performance and photovoltaic parameters, making the hysteresis effect one of the major challenges hindering the commercialization of PSCs [6].

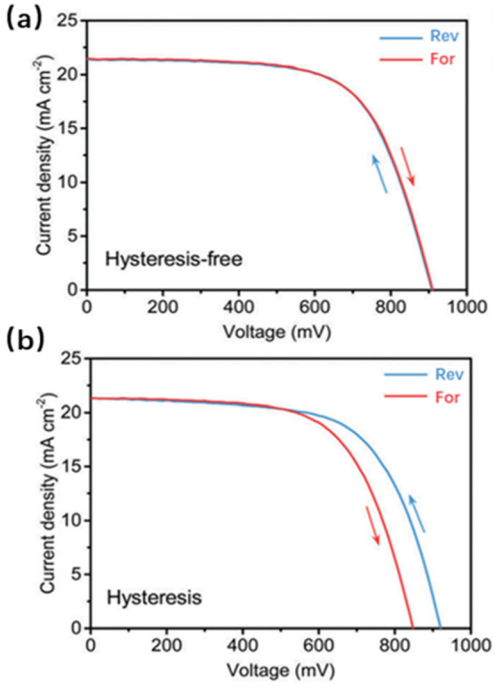

Fig. 2. Hysteresis effect in perovskite solar cells. Forward-scanned represents 300 mV → 1300 mV, whereas reverse-scanned reflects the opposite [7].

Several speculations including ferroelectric polarization [8], the trapping and de-trapping of charge carriers [9], as well as ion redistribution [10] have been proposed to understand the origin of the hysteresis effect. However, it appears that a consensus has already been established, attributing the principle cause of the hysteresis effect to the interfacial accumulated ions due to ion migration.

Perovskite is proven to have a soft lattice with a low crystallization formation energy, meaning the chemically bonded ionic components are readily released as mobile ions [11]. Subsequently, the migration of ions can be triggered by the electric field generated by photogenerated carriers, which may lead to the creation of vacancy states serving as charge traps that capture and hold photogenerated carriers, ultimately interfering with the dynamics of the charge carriers as well as the hysteresis effect. Moreover, the interfacial accumulated ions would establish another migration-induced electric field that hampers efficient charge transportation, proving detrimental to PCEs and ultimately introducing the hysteresis effect.

Typical anions that have the potential to migrate in perovskite material are usually halide ions. Typical cations that could potentially migrate in perovskites include organic cations such as methylammonium (MA^+), formamidinium (FA^+) and cesium (Cs^+). It has been proven that compensation and synergetic inhibition effects would appear if either mobile species were reduced. Therefore, an interfacial modification strategy adopting halide engineering was proposed to prepare in situ accumulated interfacial halide ions at the ETL interface, aiming at inhibition or elimination of the hysteresis effect in fabricated PSCs [12].

As such, it can be hypothesized that the elimination of ion migration would effectively inhibit the hysteresis effect, resulting in a unique PCE, greater stability, and improved overall PSC performance. This would aid in paving the way for the global commercialization of perovskite devices as a solution to the global climate and energy crises.

The purpose of this research project is to propose a strategy to eliminate the hysteresis effect in PSCs, while explaining the fundamental principles that induce the hysteresis effect in PSCs. The primary goals are to achieve the elimination of the hysteresis effect in PSCs via halide engineering, as well as establishing a correlation between the intensity of the hysteresis effect and the modifications of halide engineering (i.e. steric size and affinity gradient); this will effectively illustrate the mechanisms that cause the hysteresis effect in PSCs.

II. Experimental Design

A series of control perovskite devices without interfacial modification were prepared, and the basic optical and optoelectronic properties were measured. These results were then compared to a set of modified devices.

A. Control Device Fabrication

The standard PSC fabrication process is adopted for this experiment, involving 5 different steps:

1) Transparent Conductive Oxide (TCO) Glass Substrate Cleaning (Front)
2) Electron Transport Layer (ETL) Preparation
3) Perovskite Active Layer Preparation
4) Hole Transport Layer (HTL) Preparation
5) Metal Electrode Evaporation (Back)

The fabrication of the control device follows a traditional one-step spin coating procedure, although spray-coating may be used as well. Indium Tin Oxide (ITO) was chosen for the front TCO glass substrate, while gold (Au) was chosen for the back metal electrode of the PSC device.

Firstly, the TCO glass substrates were cleaned using detergent, acetone, deionized water and ethanol sequentially in an ultrasonic cleaner. A plasma treatment was also necessary to further enhance interfacial contact. Next, the precursor solution (SnO_2 aqueous solution) for the ETL was applied onto the TCO glass substrate using a spin coater. The precursor solution for the perovskite active layer was obtained by dissolving Methylammonium Iodide (MAI) and lead iodide (PbI_2) in a Mixture of Dimethylformamide (DMF) and Dimethyl Sulfoxide (DMSO) solvent, and was applied to the ETL via spin coating. A thermal annealing process was also necessary for enhanced crystalline quality. The precursor solution for the HTL consisted of several chemicals including Spiro-OMeTAD, bis-trimethanesulfonhydro imide, FK 209 Co(III) TFSI salt, and 4-tert-Butylpyridine, which were dissolved in their corresponding solvents before mixing them with specific recipes and applying to the perovskite active layer by spin coating. Finally, an 80 nm thick gold (Au) electrode was evaporated to complete the device fabrication process.

B. ETL Interfacial Modification via Halide Engineering for Hysteresis Inhibition

Ion migration has been identified as the primary cause of the hysteresis effect, as it results in the interfacial accumulation of ions. Therefore, the proposed strategy incorporates interfacial and halide engineering as a means of modifying the

ETL interface.

Specifically, the proposed methodology involves selecting halide salts (InX_3), namely InF_3, $InCl_3$, $InBr_3$, and InI_3, according to their respective ionic sizes and affinities. The interfacial modification is performed by mixing the selected chemicals with the ETL precursor when preparing the ETL. The pre-prepared interfacial halides will help to establish a pre-built-in electric potential in the opposite direction of the migrating ions, thus hindering the rate of ion migration, and subsequently the hysteresis effect. This migration process is correlated to both the ionic size and affinity strength of the modified ions, as illustrated in Fig. 3. The design is summarized in Fig. 4 for a comprehensive and convenient understanding of the proposed strategy.

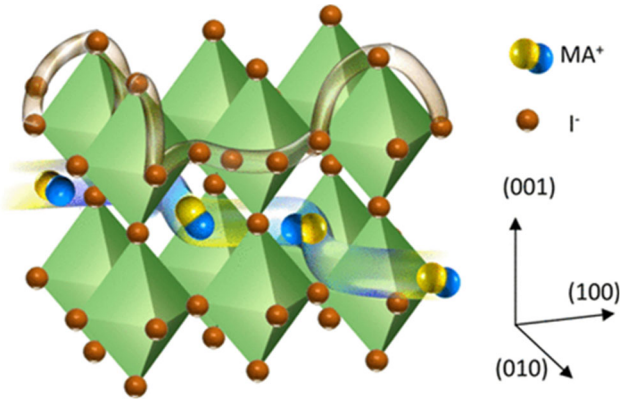

Fig. 3. Potential migration channels for various mobile ions. $MAPbI_3$ is used as an example [13].

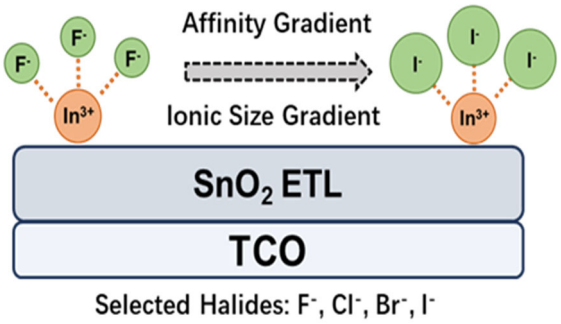

Fig. 4. Scheme 1: Schematic graph depicting the interfacial modification strategy adopting halide engineering.

Halides are chosen as they are intrinsic to perovskite material, preventing the introduction of any unwanted problems. They also exhibit the highest electronegativities and electron affinities, thus creating a stronger electric potential to inhibit the movement of mobile ions. Indium (In^{3+}) is chosen as it forms Indium Tin Oxide (ITO) when mixed with the ETL precursor solution of tin oxide (SnO_2). ITO is the most commonly-used doping ion for TCO, thus ensuring excellent compatibility with the ETL material and guaranteeing sufficient interfacial contact between the additive and the ETL.

The ETL (which influences anions) is chosen rather than the HTL (which influences cations) as anions are more likely to migrate than cations due to their lower formation energy (atoms generally have a higher affinity for gaining electrons (electron affinity) compared to losing them). Moreover, the ETL interface is chosen for ease of fabrication, but any interface can be modified to inhibit the hysteresis effect.

C. Characterizations

Certain measurements will be employed to gather basic spectrum information regarding the PSC device.

Absorption Spectroscopy. The absorption spectroscopy allows us to determine the bandgap energy of the perovskite material, which dictates the range of wavelengths of light that can be absorbed by the material, and is crucial in evaluating the overall performance of the device.

X-Ray Diffraction (XRD). The XRD utilizes an x-ray and its diffraction properties to determine crystal structure and quality as well as phases and defects of the perovskite material.

Intrinsic Photoluminescence (PL). The PL spectroscopy provides further information associated with defects and trap states, and their impacts on the radiative recombination of electron-hole pairs, which are indicators for overall performance estimation.

Time-Resolved Photoluminescence (TRPL). The TRPL will be obtained by using the Time-Correlated Single Photon Counting (TCSPC) technique to measure the charge carrier dynamics, specifically regarding excited charge carrier recombination in the PSC device, which is one of the determinant factors for efficient PCE of perovskite devices.

a) J-V curve measurements for hysteresis effect evaluation

The *J-V* measurements are the standard method used to extract the power output efficiency of a photovoltaic device, which is represented by the maximum power point (P_{max}) on the curve, as well as its PCE. The PCE is obtained by calculating the ratio of the P_{max} to the incident light power density. In perovskite devices, the PCE under different voltage scanning directions will be different. Therefore, the hysteresis effect is estimated by the Hysteresis Index (HI), which is defined as follows:

$$HI = \frac{PCE_{(Reverse)} - PCE_{(Forward)}}{PCE_{(Reverse)}} \quad (1)$$

The HI is crucial for the research project, as it will be used as the criterion to estimate the hysteresis effect with and without the proposed interfacial modification strategy, and will help to explain the potential mechanism of the hysteresis effect accompanied by Open-Circuit Voltage Decay (OCVD) measurements.

Notes: As mentioned previously, the forward-scanned *J-V* curve scans the direction of voltage increasing from a negative to positive value, whereas the reverse-scanned *J-V* curve scans the direction of voltage decreasing from a positive to negative value.

b) Open-Circuit Voltage Decay (OCVD) measurements for evaluation of mobile ion related charge carrier dynamics

The OCVD is used to measure the transient voltage decay of the PSC device, which provides information about the recombination kinetics of charge carriers. While the slow, long-lived species have been attributed to the voltage contribution from the interfacial accumulated mobile ions, the dynamic properties of the ion-related species will be used to estimate the influence on the hysteresis effect after interfacial modification under the halide engineering strategy.

III. Results and Discussion

A. Absorption Spectroscopy

In Fig. 5, there are five absorption curves. The black curve represents the control perovskite device without any halide modifications, displaying conventional perovskite absorption properties. The colored curves represent each of the modified perovskite devices as indicated by the figure legend. There is also a band gap energy of around Eg (eV) = 1240/λ = 1.59 eV, which is typical of perovskite devices. Post-modification, there is a slight blueshift towards shorter wavelengths, as well as a decrease in absorption intensity. However, the InF_3 device showcased the greatest absorption, similar to the control device. Moreover, the absorption edge, located at around 780 nm, indicates that the InF_3 device had the greatest blueshift of all the modified devices. This effectively translates to a higher crystallinity as well. This property is also related to the photoluminescence and trap state properties of the perovskite device.

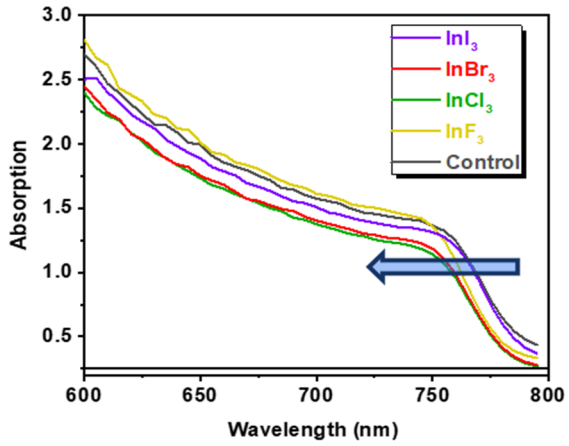

Fig. 5. Absorptions of the control and modified perovskite devices.

B. X-Ray Diffraction (XRD)

In Fig. 6, the characterization showcases two significant diffraction peaks, located at 14.7° and 28.2°, for each device. These two peaks are defining features of a well-fabricated perovskite device, and can be evaluated at the preferred orientations of (100) and (200). Overall, there is an increase in diffraction intensity post-modification. A stronger diffraction intensity also translates to higher crystallinity, which is a beneficial property of perovskite devices. The InF_3 device, like the other modified devices, had an increase in diffraction intensity. However, in all of the other devices, there exists a tiny peak at around 13°, representing the existence of unreacted PbI_2 in the perovskite device. In contrast, there is no observable peak in the InF_3 device, indicating the limitation of unreacted PbI_2 in the perovskite device. This effectively translates to a higher crystallinity as well.

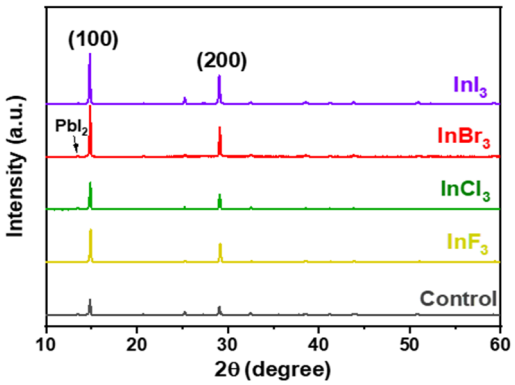

Fig. 6. XRD patterns of the control and modified perovskite devices.

C. Photoluminescence (PL) Spectroscopy

In Fig. 7, the PL emission center is around 770 nm, similar to the absorption edge of 780 nm, representing a small Stokes shift. Furthermore, the spectroscopy displays an increase in PL intensity post-modification, translating to enhanced radiative emission and passivated defects and trap states. The InF_3 device had the highest PL emission intensity, representing a well-fabricated perovskite device.

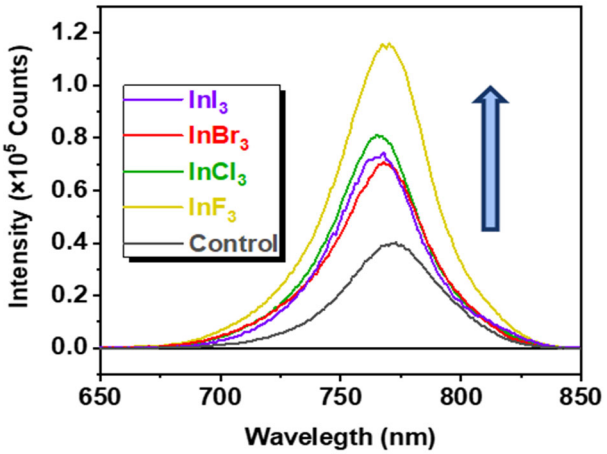

Fig. 7. PL intensities of the control and modified perovskite devices.

D. Time-Resolved Photoluminescence (TRPL) Spectroscopy

Another traditional method to evaluate the film properties of the perovskite device is the TRPL spectroscopy, as shown in Fig. 8. The TRPL spectroscopy displays dynamics of the excited charge carrier recombination in the intrinsic perovskite film (meaning ion migration is not at play here). The TRPL decay traces are shown for each perovskite device, where there is an exponential decay of the control device. Post-modification, the decay is slowed, indicating a decrease in trap state densities. Prolonged charge carrier lifetime is also observed post-modification. Notably, the InF_3 device had the longest lifetime of all the perovskite devices.

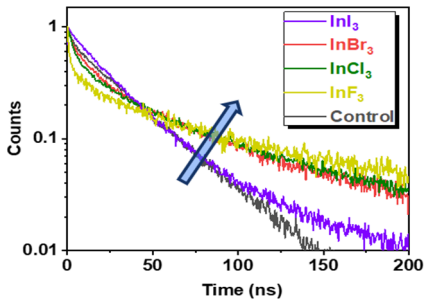

Fig. 8. TRPL decay traces of the control and modified perovskite devices.

E. Open-Circuit Voltage Decay (OCVD)

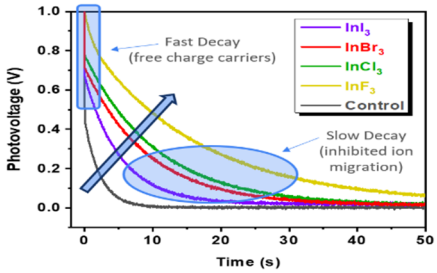

Fig. 9. OCVD graph of the control and modified perovskite devices.

The OCVD graph in Fig. 9 displays dynamics of the excited charge carrier recombination in the entire device, meaning ion migration is at play here. There are two decay components as recorded in the OCVD graph. Fast decay is related to the free charge carrier recombination, while slow decay is in terms of the ion-related decay process. The graph indicates that the ion migration-related decay slows down due to inhibited mobile ions. Overall, InF_3 device had the slowest decay. This aligns with previous results obtained from the TRPL spectroscopy.

F. Photocurrent Density-Voltage (J-V) Curves

From Fig. 10, it is easy to visualize that the control device has a significant hysteresis effect. This is largely due to the wide discrepancy between the forward- and reverse-scanning curves of the *J-V* characterization. Post-modification, this discrepancy is diminished, with the InF_3 device emerging with the least hysteresis of all the perovskite devices.

J-V curves can be used to visualize the intensity and magnitude of the hysteresis effect in perovskite devices. However, they do not accurately provide researchers with a number to measure and quantify. This necessitates the use of the hysteresis index.

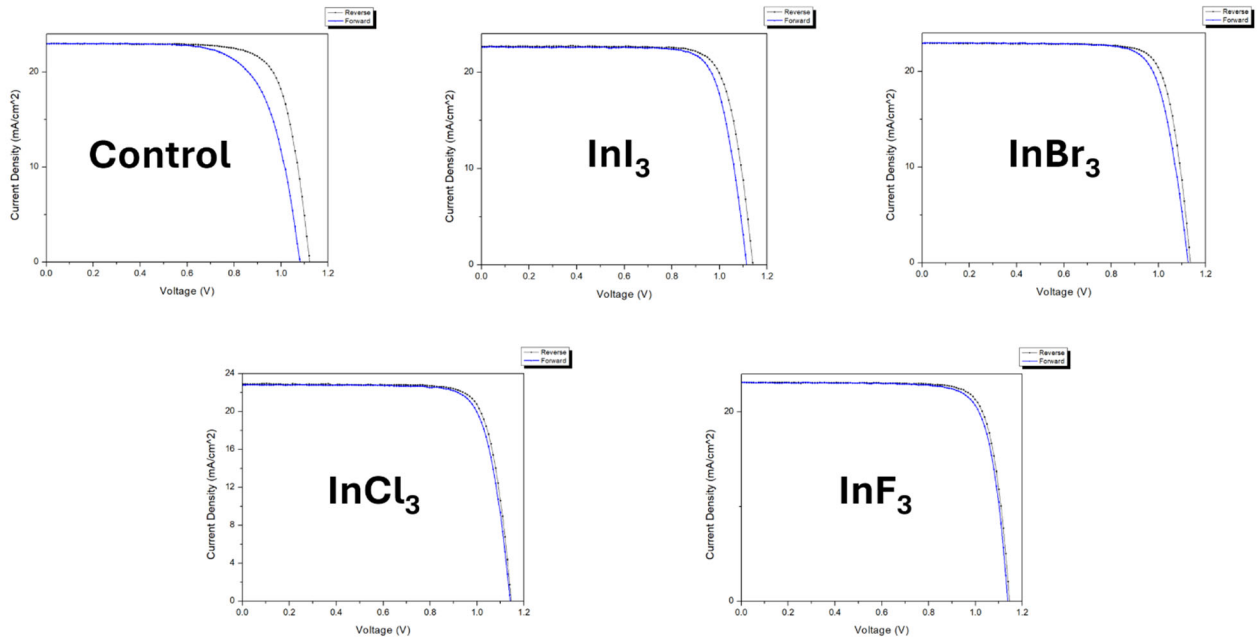

Fig. 10. *J-V* characterizations of the control and modified perovskite devices.

G. Hysteresis Index (HI) Graph

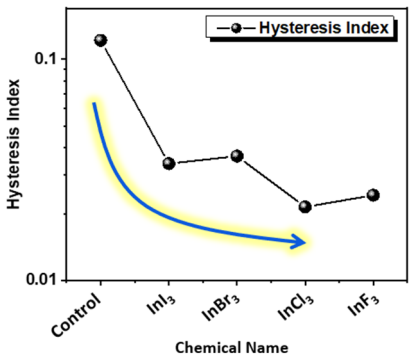

Fig. 11. HI graph of the control and modified perovskite devices.

The HI graph utilizes the HI formula to quantify the hysteresis effect. From Fig. 11, it can be observed that halides with smaller ionic sizes and higher electron affinities exhibited decreased hysteresis. However, smaller ions should be more mobile and thus exhibit greater hysteresis, indicating the importance of electron affinity in inhibiting ion migration, and thus the hysteresis effect. This will be explained further in the next section.

IV. Discussion and Conclusion

The results from the *J-V* curves indicate that the hysteresis effect was significantly inhibited post-modification. This proves the initial hypothesis correct, as the inhibition of ion

migration effectively led to decreased hysteresisTherefore, since the proposed halide engineering strategy works, it should be implemented in all future PSC fabrication methods to improve the commercial viability of perovskite devices.

More importantly, it was initially thought that ionic size played a key role in inhibiting ion migration, where larger ions would be less mobile than smaller ions. However, the results from the *J-V* curves indicate that InF_3 had the most inhibited hysteresis effect, despite fluorine having the smallest ionic size. This is likely due to fluorine having the highest electron affinity. As a result, while ionic size matters, electron affinity plays a more significant role in inhibiting ion migration, and thus the hysteresis effect in PSCs.

While it was initially thought that only the hysteresis effect would be inhibited following the modifications, basic optical and transient optoelectronic spectroscopies displayed improvements in the fundamental properties of the PSC device. This indicates that the proposed strategy is suitable not only for the inhibition of the hysteresis effect, but also for the overall improvement of PCE and PSC performance.

Conducting measurements that help to visualize ion migration including Time-of-Flight Secondary Ion Mass Spectrometry (ToF-SIMS) and Photoluminescence (PL) Imaging is a potential improvement. These measurements would identify specific migrating ions and their respective dynamics (i.e. speed, direction, location, etc.) within the perovskite device, potentially aiding in the development of more effective strategies.

Conducting research comparing the interface engineering strategy with other methods such as composition engineering and additive engineering would also prove crucial in determining the most effective strategy for inhibiting the hysteresis effect. Moreover, while PSCs exhibit the most severe hysteresis effect, other solar cells have shown milder hysteresis effects that can still interfere with power output, PCE, and the overall performance of the device. As a result, experimentation with other types of solar cells would determine whether the proposed strategy is universally applicable, with the same degree of effectiveness for all photovoltaic technologies.

Conflict of Interest

The author declares no conflict of interest.

Reference

[1] S. Schlömer. (Nov. 2023). Technology-specific cost and performance parameters. [Online]. Available: https://www.ipcc.ch/site/assets/uploads/2018/02/ipcc_wg3_ar5_annex-iii.pdf

[2] Y. Wang, P. Shen, and J. Liu *et al.*, "Dynamic performance and stability of perovskite solar cells under constant illumination," *Solar RRL*, vol. 3, 1900181, 2019.

[3] C. Liu, Y. B. Cheng, and Z. Ge, "Recent advances in flexible and stretchable organic solar cells," *Chem. Soc. Rev.*, vol. 49, pp. 1653–1687, 2020.

[4] Q. Jiang, X. Zhang, and J. You, "Sn-based perovskite solar cells: An emerging lead-free alternative," *Small*, vol. 14, 1801154, 2018.

[5] H. S. Vogelbaum and G. Sauvé, "Advances in conjugated polymer synthesis for organic photovoltaics," *Synthetic Metals*, vol. 223, pp. 107–121, 2017.

[6] W. Zhu, S. Wang, X. Zhang, A. Wang, C. Wu, and F. Hao, "Recent developments in all-inorganic perovskite solar cells: Challenges and opportunities," *Small*, vol. 18, e2105783, 2022.

[7] Y. Rong, Y. Hu, and S. Ravishankar, "Interface engineering in perovskite solar cells for enhanced stability and efficiency," *Energy Environ. Sci.*, vol. 10, pp. 2383–2391, 2017.

[8] T. Zhang, C. Hu, and S. Yang, "Recent progress in interface engineering of perovskite solar cells," *Small Methods*, vol. 4, 1900552, 2019.

[9] O. Almora, M. Garcia-Batlle, and G. Garcia-Belmonte, "Analyzing the recombination mechanisms in perovskite solar cells," *J. Phys. Chem. Lett.*, vol. 10, pp. 3661–3669, 2019.

[10] Z. H. Ai, D. H. Wu, and T. S. Ma *et al.*, "Recent advances in stability enhancement of perovskite solar cells under operational conditions," *Solar RRL*, vol. 6, 2200606, 2022.

[11] Y. Fu, H. Zhu, J. Chen, M. P. Hautzinger, X. Y. Zhu, and S. Jin, "Recent advances in metal halide perovskite photovoltaics: A review on stability, efficiency, and synthesis," *Nat. Rev. Mater.*, vol. 4, pp. 169–188, 2019.

[12] X. Yan, W. Fan, and F. Cheng, "Advances in the design of perovskite nanocrystals for optoelectronic applications," *Nano Today*, vol. 44, 101503, 2022.

[13] Y. Yuan and J. Huang, "Organic-inorganic hybrid perovskite solar cells: A review of recent developments," *Acc. Chem. Res.*, vol. 49, pp. 286–293, 2016.